Experimental Flowfield Study on a Supercritical Airfoil

Karl A. Bütefisch* and Egon Stanewsky†
Institut für Experimentelle Strömungsmechanik, Germany

This aim of this study was to investigate the phenomenon of shock/boundary-layer interaction on a supercritical airfoil with and without shock-induced separation and to compare the results obtained by a conventional boundary-layer probe with those from a two-component Laser-Doppler Anemometer. Measurements were made in the 1×1 m^2 transonic wind tunnel (TWG) of the DFVLR Göttingen on a 250-mm-chord model of the airfoil CAST 7/DOA1 at $M_\infty=0.765$ and angles of attack of $\alpha\simeq3.6$ and 5 deg. The Reynolds number was $Re=2.5\times10^6$. Generally, the agreement between the two data sets was satisfactory. However, some discrepancies remained, especially at positions close to the wall, where the LDA data showed, in some instances, a considerable scatter. Furthermore, within the separated region where flow reversal occurs, both the LDA and the probe data are suspect.

Nomenclature

b = test section width, model span
c = airfoil chord
c_f = skin-friction coefficient
C_L = lift coefficient
c_p = pressure coefficient, $(p-p_\infty)/q_\infty$
H = shape parameter, δ^*/θ; height
H_{32} = shape parameter, δ^{**}/θ
M = Mach number
p = static pressure
q = dynamic pressure
Re = Reynolds number, $U_\infty c/\nu_\infty$
u = velocity in the boundary layer
u_τ = friction velocity, $(\tau_w/\rho_w)^{1/2}$
U^+ = velocity based on law of the wall
U_∞ = freestream velocity
x = coordinate in streamwise direction
y = coordinate normal to x
Y^+ = yu/u_τ
δ = boundary-layer thickness
δ^* = displacement thickness
δ^{**} = energy thickness
θ = momentum thickness
ν = kinematic viscosity
ρ = density
τ = shear stress

Subscripts

e = edge of boundary layer
L = local condition
w = wall
∞ = freestream conditions
1 = upstream of shock

Introduction

THERE is certainly no need to stress here the importance of the investigation of transonic flowfields to the development and design of aerodynamic flight vehicles and their components. Such flowfields may occur on transonic airfoils and wings of transport and fighter aircraft, on helicopter blades, in turbomachinery, and in the recompression region of supersonic intakes. One characteristic feature is the interaction between a near-normal shock wave, terminating the local supersonic region, and the boundary layer. This interaction determines in many instances the performance boundaries of a flight vehicle, and therefore a considerable interest in the details of this flow phenomenon and the means of its control exist.[1] Since theoretical methods do not yet perform satisfactorily, one must strongly rely on experimental results. This is particularly true with regard to shock-induced separation and the generation and/or amplification of turbulence within the interaction region. Providing the needed information requires, of course, a continuous effort in developing adequate tools. It is in that sense that a thorough investigation of the interaction field by boundary-layer probe measurements was followed by tests with a one-component forward scattering[3] and in the present study with a two-component Laser-Doppler Anemometer operating in a back-scattering mode where the signal intensities are less. The test cases are the same in all instances, providing a comparsion of two modes of LDA operation with conventional boundary-layer probe measurements.

Experimental Setup

The wind tunnel TWG[4] is a continuous closed-circuit tunnel. The test section with a cross section of $1\text{ m}\times1\text{ m}$ is operated in a Mach number range of $M_\infty=0.50$ to 1.20 at total pressures ranging from 0.25 to 1.6 bar, yielding Reynolds numbers between $Re/c\simeq3\times10^6$ to 20×10^6 m^{-1}. The settling chamber contains the probe for seeding the flow.

The present investigation was carried out on a transonic airfoil designed by the Dornier Company, CAST 7/DOA1, which has previously been used extensively for similar studies.[2,3] The airfoil is shock-free at the design point $M_\infty=0.760$, $C_L=0.573$. It is also characterized by a moderate rear loading and a relatively small trailing-edge angle (see Fig. 1).[5,6]

The model spanned the entire width of the tunnel, providing a span-to-chord ratio of $b/c=5$, which rendered the test setup essentially free of side wall interference effects. The model was equipped with 117 orifices for surface pressure measurements.

Test Conditions

Two off-design test cases were selected, one with a shock-upstream Mach number of $M_1\simeq1.30$, where shock-induced separation is incipient, and a second with $M_1\simeq1.36$, where

Received Nov. 13, 1986; revision reeived March 11, 1987.

*Head of Measurement Physics Branch.
†Acting Director.

substantial separation occurs. Mach number distributions are shown in Fig. 2; schlieren pictures are presented in Fig. 3. The boundary-layer probe and its support were removed from the test section for the LDA measurements. The probe support caused, at the lower angle of attack of $\alpha \simeq 3.5$ deg, some global interference resulting mainly in a difference in the shock location between the probe and the LDA setup (Fig. 2a). Subsequent comparisons between the probe and the LDA data will therefore be made relative to the shock location. At the higher angle of attack of $\alpha \simeq 5$ deg, only a slight difference in the rear pressure recovery exists (Fig. 2b). The slight difference in α is due to matching the lift coefficient for the two sets of measurements.

Laser-Doppler Anemometer and Boundary-Layer Probe

The LDA system was designed for application in large wind tunnels and has to fulfill the requirements of the rough environment of large facilities. In particular, it was necessary to install the device in the plenum chamber of the wind tunnel and to provide for the realignment of the optics and the laser by remote control during tunnel operation. To save wind tunnel time, fully automatic operation during a run, including the quick positioning of the measuring volume, quick data acquisition, and reduction and on-line data display, had to be established.

Figure 4 schematically shows the optical system. Two lines of an argon-ion laser are used to form two pairs of parallel laser beams of equal intensity. Passing the transmitting optics, they intersect each other at a distance of 750 mm.

Small oil particles of about 1-μ diameter, crossing the point of intersection (measuring volume) with the surrounding flow velocity partially scatter the light. The same lenses used for transmitting the laser beams collect the scattered light, which is Doppler-shifted due to the motion of the particles. The scat-

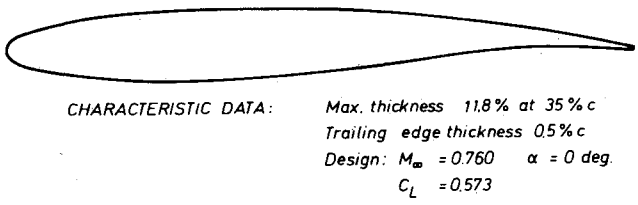

Fig. 1 The airfoil investigated.

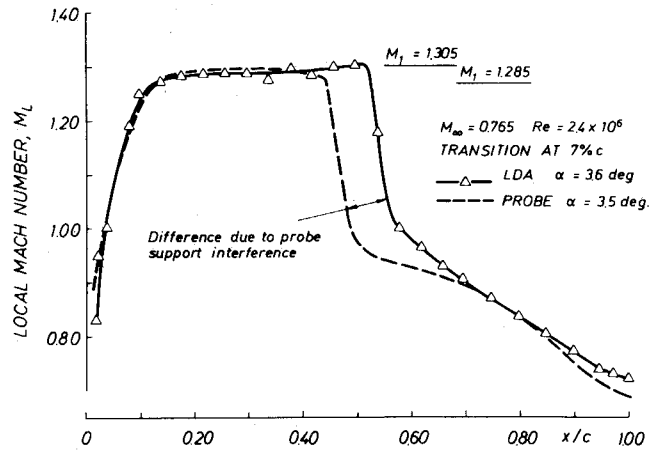

Fig. 2a Upper surface Mach number distributions at moderate incidence.

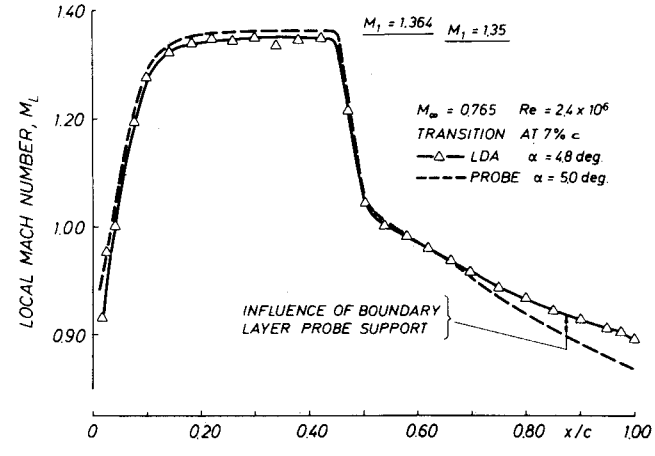

Fig. 2b Upper surface Mach number distributions at high incidence.

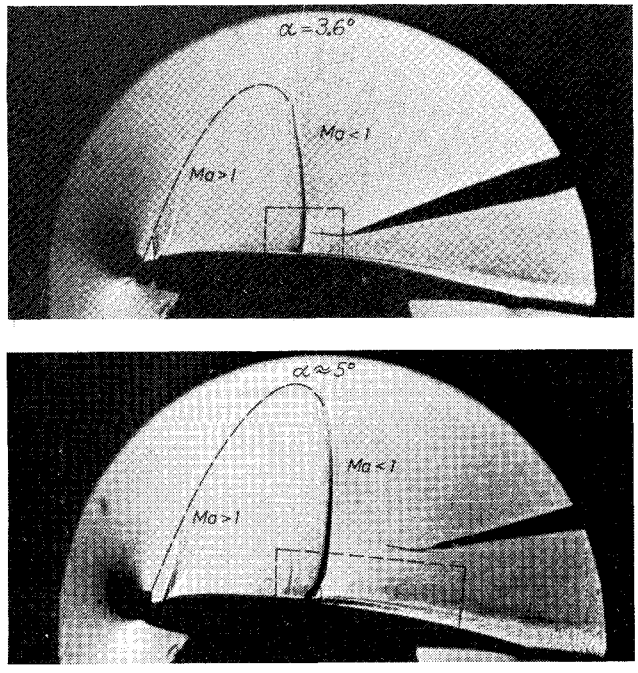

Fig. 3 Flowfield of the test cases investigated.

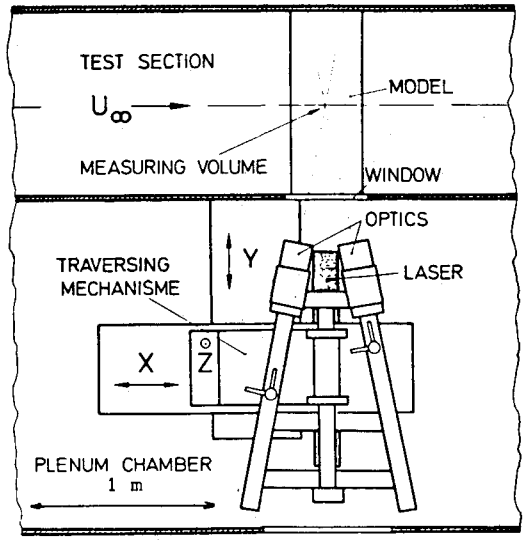

Fig. 4 LDA setup installation in the plenum chamber of the Transonic Wind Tunnel Göttingen (TWG).

tered light is passed to photomultipliers, where the Doppler frequencies, proportional to the velocity of the particles, are obtained as electrical signals. Counters convert the analog signals into digital data that are processed by a minicomputer. All optical parts were commercially acquired. However, the receiving modules had to be modified to optimize the alignment. To avoid additional mirrors, the optical axis was chosen to be nearly perpendicular to the mean flow direction. The two optical systems were installed together on a rigid X-beam construction[10] and mounted on a coordinate table to permit traversiang along the three coordinate axes in steps of 1/80 mm. For each color, one leg served as the emitting and the other as the receiving device. The advantages of this setup compared to an on-axis system are the reduction of unwanted scattered light and the decrease of the effective length of the measuring volume. Measurements in the vicinity of a wall suffer especially from scattered light, which shows up as an increase in "turbulence."

Although the mean velocity value may be influenced by the averaging procedure,[12] simple arithmetic averaging was used to obtain the mean velocity values from about 1000 samples per component. The data rate was chosen to be about 200 samples/s, leading to a measuring time of about 5 s per acquired field point.

The boundary-layer probe and its drive mechanism for the accurate positioning in the normal (y) and axial (x) direction was mounted on a sting, which, in turn, was attached to the tunnel support. This arrangement allowed the probe to always be adjusted tangential to the model surface and traversed in the direction normal to it. The probe itself consisted of a flattened pitot probe of 0.15-mm height, a cone-cylinder static probe, and a directional probe, the latter constructed of two tubes cut off under 45 deg. The overall accuracy of the probe pressure measuring system in determining the flow velocities, important in conjunction with the comparison of the probe and LDA results, was determined to be about ±2%.

The boundary-layer properties were computed from the measured static and pitot pressures, assuming a constant total temperature throughout the boundary layer. In determining the boundary-layer integral parameters, the measured velocity profiles were supplemented by the laminar sublayer, whose computation was based on the wall shear stress τ_w obtained by fitting a wall/wake profile to the measured data points assuming equal mass flux (Fig. 5).[7,8] The latter was also utilized to determine the skin-friction coefficients (see Figs. 6 and 7). A comparison of the measured and the corresponding wall/wake profile at a position well upstream of the shock has already been shown in Fig. 6.

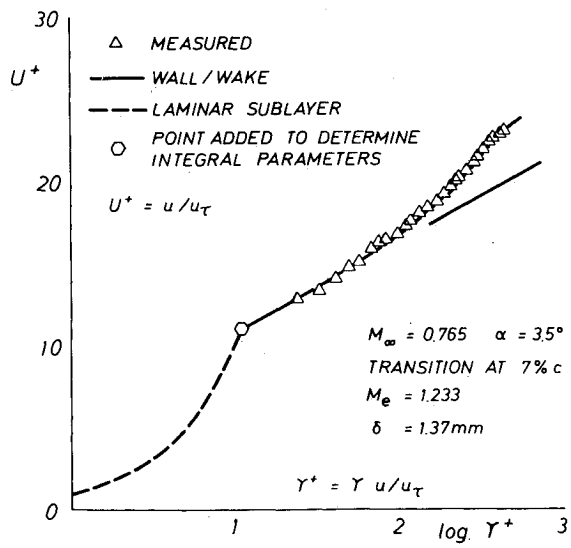

Fig. 5 Incoming boundary-layer comparison with wall/wake law profile.

The probe measurements must, in the vicinity of separation and within separated regions, be considered with caution. Since here the flow can no longer be regarded as steady and reversed flow ocurrs, the probe reading is, particularly close to the wall, erroneous, so that the boundary-layer integral parameters (e.g., c_f and δ^*) are approximations showing a trend rather than absolute values.

Discussion of Results

Emphasis in the present investigation was placed on the LDA measurements in a relatively large transonic wind tunnel at conditions of shock-induced separation and on a comparison of LDA and probe results in the shock/boundary-layer interaction region.

At the low angle of attack, the thickness of the incoming boundary layer is approximately $\delta = 1.5$ mm (Fig. 6). The shock causes an increase in the boundary-layer thickness by a factor of two and an increase in the displacement thickness by a factor of about 4.4, the latter being more pronounced due to a strong retardation of the boundary-layer profile close to the surface. The skin-friction distribution shows that the flow is not separated.

In the second test case, the shock strength is substantially higher than at the lower incidence. The corresponding boundary-layer development (Fig. 7) exhibits a much more severe thickening, with the displacement thickness now being changed by a factor of approximately 7. Furthermore, a plateau in the boundary-layer parameters, indicated in Fig. 6 for the low incidence case, no longer exists, suggesting the presence of a large shock-induced separation bubble. The latter is confirmed by the skin-friction distribution shown in Fig. 7 and by the schlieren photograph of Fig. 3. The downstream extent of the separated region can, due to the aforementioned limitations of the boundary-layer probe measurements, only be considered an approximation.

In Fig. 8, a typical velocity profile obtained for the low-incidence test case is shown. As mentioned before, the shock position has been influenced by the probe support. Taking into account the shift in the shock position of about 10%, the probe and LDA profiles have been plotted together. The

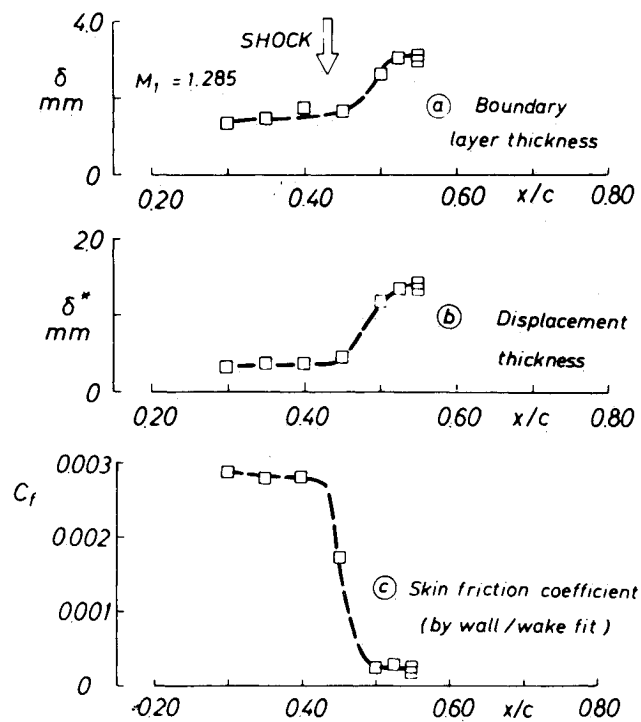

Fig. 6 Boundary-layer parameters for moderate incidence.

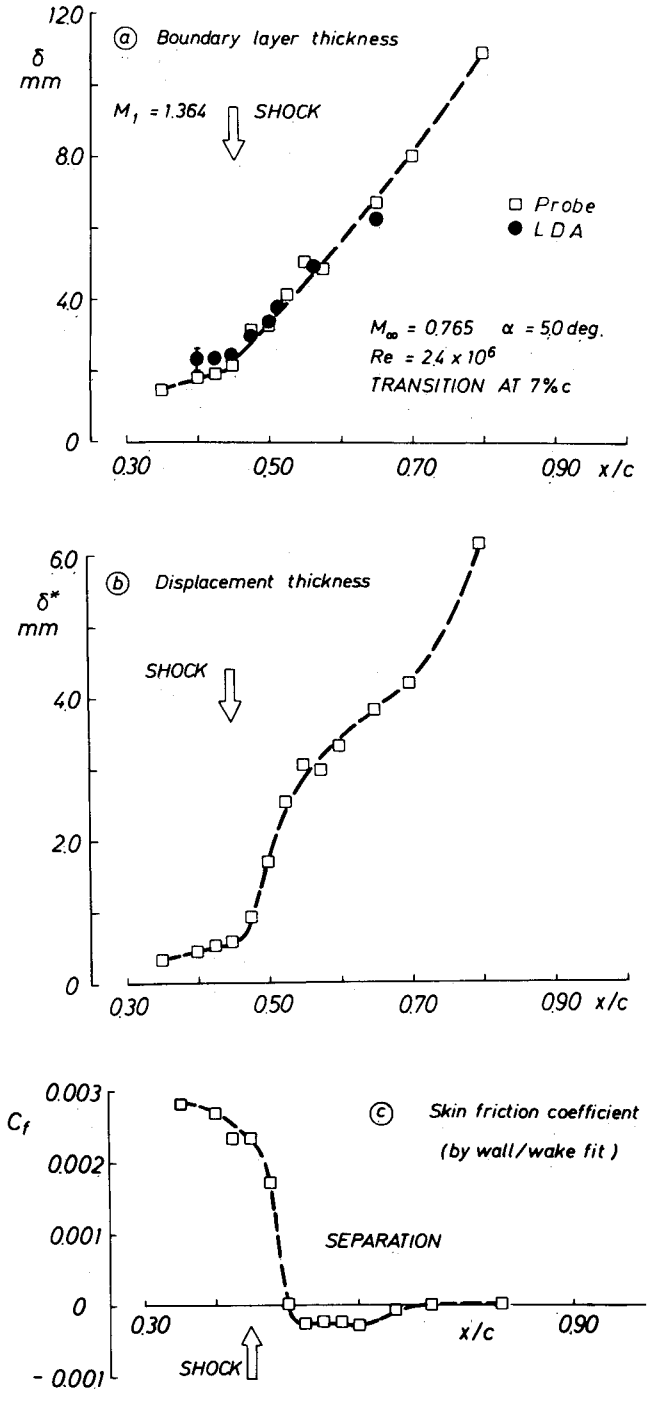

Fig. 7 Boundary-layer parameters for high incidence.

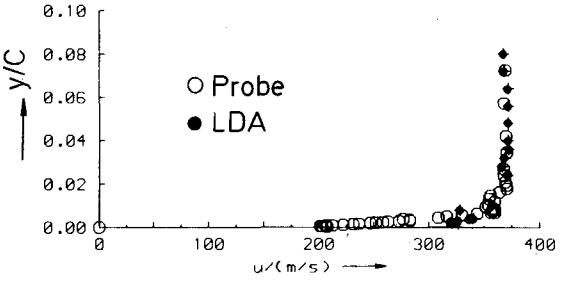

Fig. 8 Velocity profiles within the shock layer, comparison probe/LDA results; $\alpha = 3.6$ deg, $x/c = 55\%$.

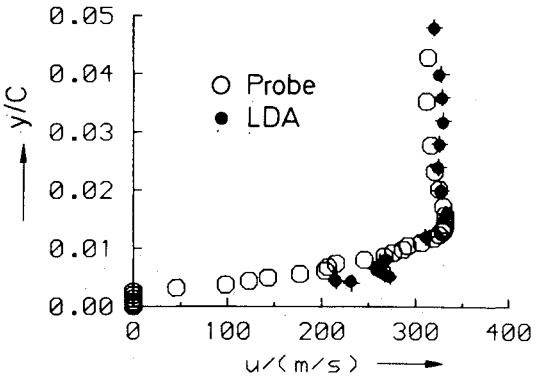

Fig. 9 Velocity profiles in the shock/boundary-layer interaction regime, comparison probe/LDA results; $\alpha = 5$ deg, $x/c = 50\%$.

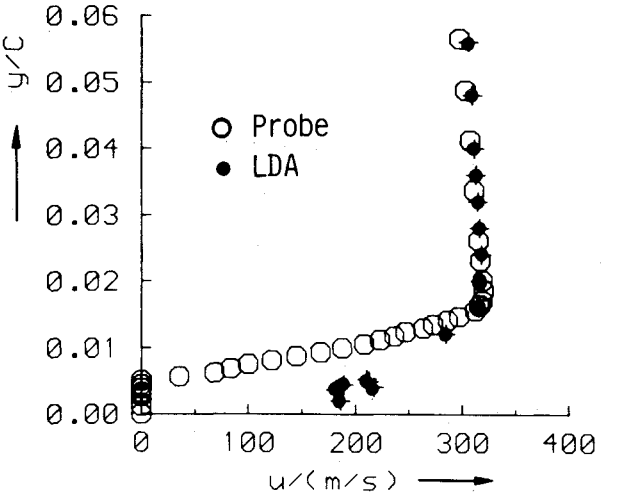

Fig. 10 Velocity profiles in the shock/boundary-layer interaction regime, comparison probe/LDA results; $\alpha = 5$ deg $x/c = 52\%$.

agreement is quite good in the outer flowfield; however, very close to the wall, the LDA data show a large amount of scatter. This seens mainly due to the vibrations of the model during the tests. These vibrations were particularly pronounced in the midspan of the model where the measurements took place. Also note that the measurements were taken within the immediate shock region.

The comparison of boundary-layer profiles obtained by LDA and the boundary-layer probe for the high-incidence test case shows, upstream of and some distance into the interaction region, a good overall agreement between the two data sets, which results in good agreement in the predicted boundary-layer thicknesses (Fig. 7). At $x/c = 50\%$ (Fig. 9), the probe data indicate the beginning of a separation bubble and a deceleration of the flow as the probe moves away from the wall through the complex lambda-shock system. The LDA data also indicate the closeness to separation; however, the detailed outer structure is not indicated. This may be due to the intrinsic shock oscillations seen by the LDA but somewhat subdued by the presence of the probe. At $x/c = 52\%$, the outer flow is again well predicted by the LDA in agreement with the probe measurement (Fig. 10). Differences occur within the separated boundary layer. These may be due to the probe readings being erroneous at these conditions as well as the LDA not being sensitive to the flow direction, since Bragg cells were not used.

Figure 11 shows the present LDA result for $\alpha = 5$ deg in comparison with the published LDA and probe data of Ref. 3.

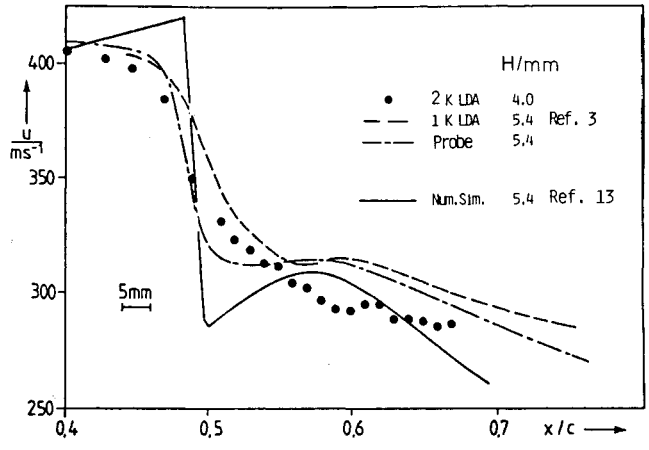

Fig. 11 Velocity profiles across the shock.

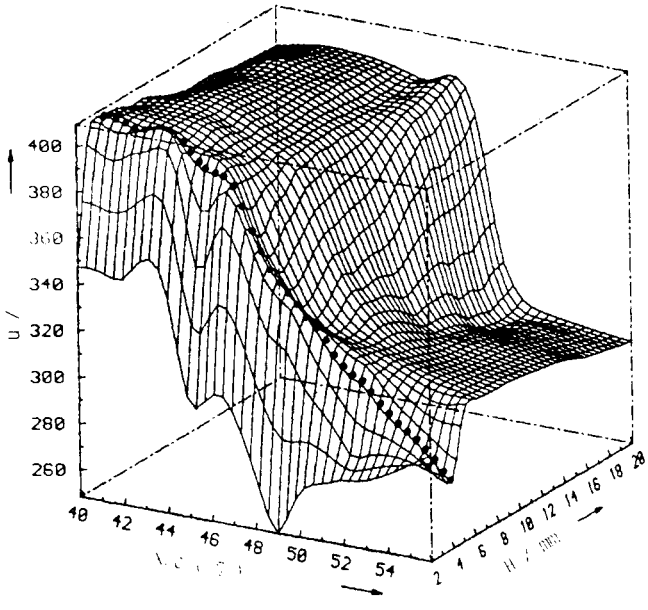

Fig. 12 Three-dimensional velocity carpet plot of the two-component LDA measurements, $\alpha = 4.8$ deg.

The velocity gradient indicated by the present data is comparable to the one shown by the one-component LDA results but does not confirm the steeper slope determined by the boundary-layer probe. One reason may be that the position of the shock fluctuates by a small amount and LDA data show as a result a spreading of the pressure rise, whereas the solid pressure probe, as mentioned earlier, fixes the shock position.

On the other hand, the distances from the wall are slightly different, with the present LDA being closer to the wall where the pressure rise due to the shock is spread over a larger chordwise distance. This would also explain the lower velocities downstream of the shock. In order to demonstrate the effect of small changes in location, all measured LDA velocities are presented in a three-dimensional carpet plot obtained by a three-dimensional spline interpolation (Fig. 12). Clearly, a considerable change of the velocity profile behind the shock is noted when changing the distance from the wall from $H = 4.0$ (dotted line) to 5.4 mm.

The two-component LDA measurements provide additional flow properties, such as the flow direction and the turbulence levels. Figure 13 shows the chordwise velocity profiles across the shock for the two test cases. A pronounced change in

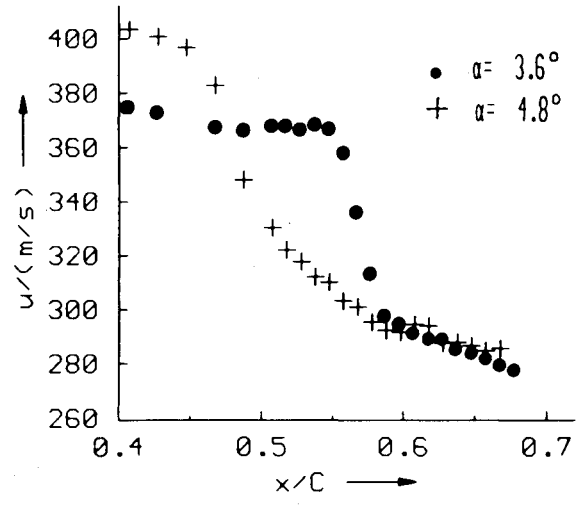

Fig. 13 Chordwise velocity profiles across the shock.

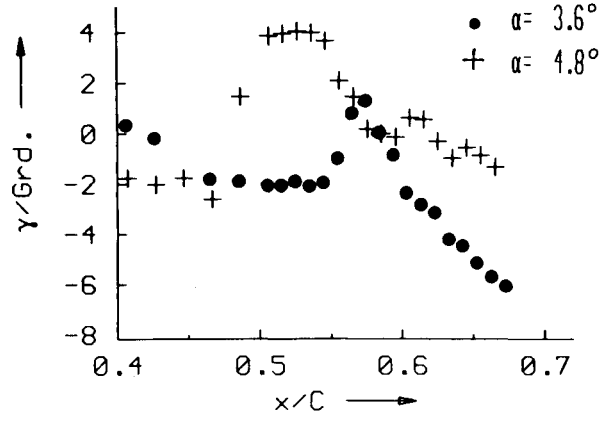

Fig. 14 Change of the flow angles across the shock.

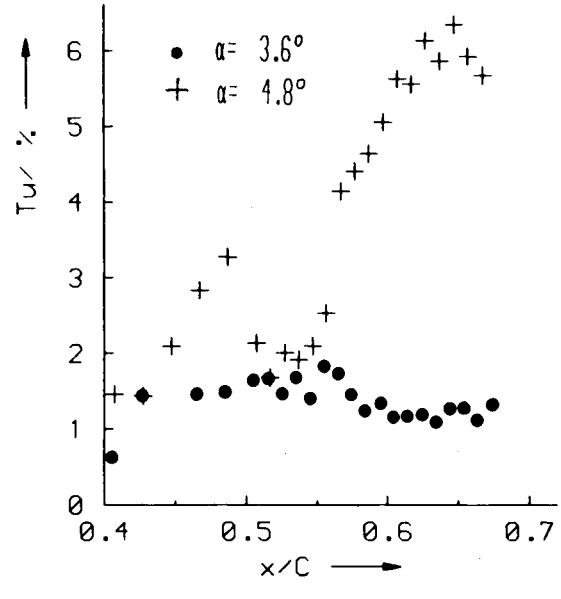

Fig. 15 Turbulence profiles across the shock.

shock structure is indicated as the angle of incidence is increased. The measured flow angle distributions in Fig. 14 reflect the change in the boundary-layer thickness due to the interaction of the boundary layer with the shock, also indicating the separation region at the higher angle of incidence. The corresponding turbulence data, which still contain some artificial noise, are presented in Fig. 15. At the low incidence, the shock hardly affects turbulence. At $\alpha \simeq 5$ deg, two regions of higher turbulence can be recognized: the first one immediately at the shock, possibly due to shock oscillations, the second associated with the reattachment process (also see Fig. 7c).

Conclusion

A two-component Laser-Doppler Anemometer operating in back-scatter mode was applied in the 1×1 m^2 transonic wind tunnel to analyze the shock/boundary-layer interaction region on a transonic airfoil. The LDA data were compared to conventional boundary-layer probe results. As a clear advantage of the LDA, one can state its ability to measure non-intrusively, thus avoiding changes, for instance, in the shock behavior, which obviously occur due to the presence of the solid probe. Furthermore, more detailed information, such as the turbulence level and the Reynolds shear stresses, can be obtained simultaneously with the mean flow properties. The investigation has also shown that the present technique must be improved: Bragg cells must be incorporated to determine the flow direction, and the instantaneous position of the model must be recorded and related to the position of the measuring volume.

Acknowledgments

The authors would like to thank Mrs. I. Redlin, Mrs. I. Nickisch, and Mrs. U. Dreykluft for preparing the manuscript.

References

[1]Stanewsky, E., and Krogmann, P., "Transonic Drag Rise and Drag Reduction by Active/Passive Boundary Layer Control," AGARD-R-723, July 1985, pp. 11-1–11-41.

[2]Stanewsky, E., "Interaction between the Outer Inviscid Flow Field and the Boundary Layer on Transonic Airfoils," Doctoral Thesis D83, Technical University Berlin, 1981.

[3]Schäfer, H.J., Horny, G., Pfeiffer, H.J., and Stanewsky, E., "Applicability of the Laser-Doppler-Anemometry to the Investigation of the Transonic Interaction between a Shock and the Boundary Layer," Rept. R 131/83, Deutsch-Französisches Forschungsinstitut Saint-Louis, July 1983.

[4]Hottner, T. and Lorenz-Meyer, W., "Der Transsonische Winkanal der Aerodynamischen Versuchsanstalt Göttingen (Zweite Ausbaustufe)," Jahrbuch 1986 der WGL, 1968.

[5]Kühl, P. and Zimmer, H., "The Design of Airfoils for Transport Aircraft with Improved High Speed Characteristics," DORNIER GmbH. Rept. 74/16 B, 1974.

[6]Stanewsky, E. and Zimmer, H., "Design and Wind Tunnel Testing of Three Supercritical Airfoils for Transport Aircraft," Z. Flugwiss, Vol. 23, 1975, pp. 246–256.

[7]Stanewsky, E. and Thiede, P., "Boundary Layer and Wake Measurements in the Trailing Edge Region of a Rear-loaded Transonic Airfoil," *Viscous and Interacting Flow Field Effects,* Research Rept. FBWT 79-31, German Ministry of Defense, 1979.

[8]Mathews, D.C., "Shock Wave-Boundary Layer Interactions in Two-dimensional and Axially-symmetric Flows Including the Influence of Suction," Ph.D. Thesis, University of Washington, 1969.

[9]Bütefisch, K.A. and Strunck, V., "A Two Component LDA-System to be Operated in a 3m × 3m Low Speed Wind Tunnel," *Proceedings of the Symposium on Applications of Laser Anemometry to Fluid Mechanics,"* Lisbon, Portugal, July 1984, p. 10.3.

[10]Sauerland, K.-H., "Entwurf eines 3-Komponenten LDA Systems für den Transsonischen Windkanal der DFVLR in Göttingen," LDA Meeting ISL, ONERA, DFVLR, 1983.

[11]Durst, F., Melling, A., and Whitelaw, I.H., "Principles and Practice of Laser Doppler Anemometry," Second ed., Academic Press, London, 1981.